# THERMAL COMFORT LEVELS IN A CONDITIONED ENVIRONMENT WITH DISPLACEMENT VENTILATION AND RADIANT COOLING FLOOR CALCULATED USING COMPUTATIONAL FLUID DYNAMICS

Peña-Suárez J.M. and Ortega-Casanova J.*
*Author for correspondence
E.T.S. Ingeniería Industrial. Andalucía Tech.
University of Málaga,
Málaga,
Spain,
E-mail: jortega@uma.es

## ABSTRACT

In a society in continuous development, the requirements for thermal comfort and indoor air quality are increasing. However, these should be achieved by rational energy consumption. With this in mind, the combined use of displacement ventilation (DV) and radiant cooling floor (RCF) is an innovative concept that has become popular as a cooling system in high-rise public enclosures.

To provide a high thermal comfort, the effects of buoyancy, supplied air temperature, air discharge angle and surface floor temperature should be treated with special care.

Therefore, this paper presents a sensitivity analysis considering these critical parameters in different numerical simulations. The results of the simulations are used to calculate the thermal comfort index, according to ISO 7730 standard, in high ceiling enclosures using a DV + RCF system. The general thermal sensation has been predicted using the *PMV* (Predicted Mean Vote) and *PPD* (Predicted Percentage of Dissatisfied) indices. The local thermal discomfort has been evaluated by radiant temperature asymmetry, draught, vertical air temperature differences and floor surface temperatures. According to these indices, the classification of Category A is reached using DV + RCF system, exception of the radiant temperature asymmetry index. That fact will be discussed in detail, analyzed the suitability of the calculation indicates in ISO 7730 for systems involved in radiating surfaces.

## NOMENCLATURE

| | | |
|---|---|---|
| $v^*$ | [-] | Dimensionless velocity |
| $v_s$ | [m/s] | Mean air velocity at the diffuser exit |
| $\|v\|$ | [m/s] | Magnitude of the air velocity |
| $A_l$ | [m$^2$] | Lateral area of the diffuser |
| $A_{eff}$ | [m$^2$] | Effective discharge area of the diffuser |
| $K$ | [-] | Percent of the diffuser lateral area considered as effective |
| $Ar$ | [-] | Archimedes number |
| $h$ | [m] | Height of the diffuser |
| $D$ | [m] | Outer diameter of the diffuser |
| $L_c$ | [m] | Characteristic length of the diffuser |
| $D_{influence}$ | [m] | Maximum distance of influence of a diffuser |
| $T_s$ | [ºC] | Air temperature supplied by the diffuser |
| $T_f$ | [ºC] | Floor temperature |
| $\Delta T_{s-f}$ | [ºC] | Temperature difference between the air supplied by the diffuser and the floor surface |
| $g$ | [m/s$^2$] | Gravity acceleration |
| $[r, \theta, z]$ | [m, -, m] | Cylindrical coordinates |
| $PMV$ | [-] | Predicted Mean Vote |
| $PPD$ | [%] | Predicted Percentage of Dissatisfied |

Special characters

| | | |
|---|---|---|
| $\rho$ | [kg/m$^3$] | Air density |
| $C_p$ | [J/kgK] | Air specific heat |
| $\beta$ | [K$^{-1}$] | Coefficient of thermal expansion |
| $\alpha$ | [º] | Air supply angle |

Subscripts

| | |
|---|---|
| $s$ | Supply |
| $f$ | Floor |
| $l$ | Lateral |
| $eff$ | Effective |
| $c$ | Characteristic |

## INTRODUCTION

Everyday activities in industrialized countries require a prolonged stay in all types of buildings and indoor spaces. Poor quality indoor air can pose a health risk [1]. This problem has been enhanced due to a growing need for energy savings [2] which has led to the design of buildings more airtight, with greater air circulation, and therefore a possible increase of indoor air pollution.

As the importance of healthy indoor environments is recognized [3], the demand for good indoor air quality increases. However, traditional cooling systems have excessive energy consumption and do not always provide satisfactory results for solving the current problems in indoor air quality. A more economic mean of providing thermal comfort to the occupants of buildings is to use a hybrid cooling system consisting of radiant cooling floor and displacement ventilation.

The combined use of displacement ventilation (DV) [4]-[5] and a radiant cooling floor (RCF) [6] is increasingly common in the field of building climatization. Particularly in public buildings, characterized by diaphanous and high-rise spaces, where the efficiency of the hybrid cooling system increases.

On one hand, DV systems guarantee low-turbulence air supply. The air is injecting directly into the occupied zone and the discharge velocity is very low (<0.5 m/s). Depending on the degree of activity of the persons in the occupied zone, the supply air can enter the space with a temperature difference of -1 ºC to -6 ºC in relation to the room air. On the other hand, RCF systems are based on circulating cold water through a circuit of pipes embedded in the pavement. The water flow temperature is around 15 ºC, instead of the 7 ºC required in a conventional system. The hybrid cooling system (DV + RCF) combines both technologies and their advantages [7]. Only the occupied zone is treated, reaching a huge energy savings and a high comfort degree. This system is particularly recommended in high rise enclosures. The air spreads on the cold floor and is lifted by convection currents from located heat sources, so fresh and clean air remains in the lower level of the enclosure (where the occupants are located), and the relatively warmer and polluted air is located at the higher level.

A good designing and implementation of a HVAC system, aimed at saving energy, should not be detrimental with good both air quality and thermal comfort. In this paper, the degree of thermal comfort achieved with the previous hybrid cooling system is studied basing on ISO 7730 [8].

For this work, CFD (Computational Fluid Dynamics) is used to carry out the thermal comfort study in a large enclosure. The CFD technique has developed strongly from the development of computers, with increasing interest in the industrial community. It also allows to obtain in a reasonable time a huge amount of information that otherwise would require the dedication of enormous human and material resources, especially in the initial design phase, when the information provided by these simulations is crucial, because many changes can be made with a very low increase in the cost.

The ability to troubleshoot indoor climate control of buildings using CFD is evident in studies conducted in large rooms or public places. Specifically, the CFD technique has been used in many designs and evaluations of both thermal comfort and air quality in public buildings [9]-[10].

This paper presents calculations using numerical simulations of thermal comfort parameters in high ceiling enclosures using a DV + RCF system, including displacement diffusers and a radiant cooling floor. To that end the numerical simulations of airflow in a high-rise enclosure, including displacement diffusers and radiant cooling floor have been conducted. The purpose is to find, quickly and efficiently, the range of the environmental variables that allow achieving the highest degree of thermal comfort. This way, the hybrid cooling system is classified, according to the requirements for general thermal comfort and local thermal discomfort. The results of the simulations are used to calculate the thermal comfort index according to ISO 7730 standard. The general thermal sensation has been predicted using the *PMV* (Predicted Mean Vote) and *PPD* (Predicted Percentage of Dissatisfied) indices. The local thermal discomfort has been evaluated by radiant temperature asymmetry, draught, vertical air temperature differences and floor surface temperatures. According to these indices the classification of Category A is reached, with the exception of the radiant temperature asymmetry index. This index exclusively depends on the temperatures of the ceiling and floor and requires a temperature gradient below 5 ºC to achieve Category A.

## GEOMETRY UNDER STUDY, COMPUTATIONAL DOMAIN AND BOUNDARY CONDITIONS

The aim of this study is to analyze numerically the thermal behaviour of a DV + RCF system. To that end, the numerical simulations are performed with the commercial CFD software FLUENT [11]. The displacement ventilation units most suitable for large diaphanous enclosures are vertical cylindrical diffusers. These diffusers are located directly on the floor, uniformly distributed on the enclosure and placed at a distance equal to the twice maximum distance of influence ($2D_{influence}$), see [12]. In [12] it is also proved that the primary air stream moves at floor level and that this is the most appropriate distance. On the one hand, the distance between diffusers should not be less than $2D_{influence}$ to avoid interference the primary air streams and these interact with a velocity close to zero. On the other hand, the distance between diffuser should not be higher than $2D_{influence}$ to ensure that the supply air is in contact with the floor. The reason is that the air supplied by the diffusers receives pre-treatment dehumidification, reducing the dew point on the floor surface and prevents condensation.

Figure 1 shows a simple sketch of the studied cooling system, where the vertical cylinders indicate the locations of the DV units.

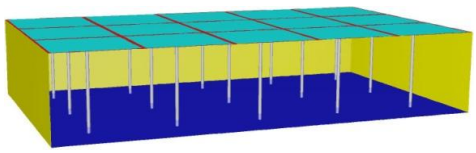

**Figure 1** Displacement diffusers uniformly distributed in a large diaphanous enclosure.

A numerical study of a complete three-dimensional enclosure including all diffusers is complex due to the large size of the domain and the high number of used diffusers. However, since each diffuser has its own zone of influence around it (see the red circle with radius ~ $D_{influence}$ in Figure 2), in order to analyze the behaviour of the whole installation only that zone of influence will be studied, instead of the entire complex domain.

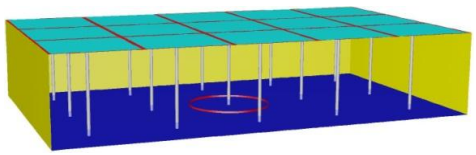

**Figure 2** Zone of influence of a diffuser.

In addition to this, the numerical simulations can be considered as two-dimensional, actually axisymmetric, if the diffuser is seen as a cylindrical body and one takes into account its azimuthal symmetry. Therefore, the simulations could be finally performed on a vertical plane placed parallel to the airflow stream, as shown in Figure 3 where the diffuser, its zone of influence (delimited by a red cylinder) and the

computational plane (the black rectangle) are shown. This plane extends from the floor to the ceiling, being 8 m high and 4 m wide ($D_{influence}$ ~ 4 m). According with this, a cylindrical coordinate system ($r$, $\theta$, $z$) is used with the origin of coordinates located at the floor and on the axis of symmetry.

The diffuser under study is similar to a commercial model with a height ($h$) equals to 0.6 m and a diameter ($D$) of 0.3 m. However, the appropriate description of air diffusers used in displacement ventilation is very complex in CFD because of the external plate perforations. Its right modelling requires a large number of nodes to properly capture the velocity profiles in each orifice, but this fact would increase the computational cost of the simulations.

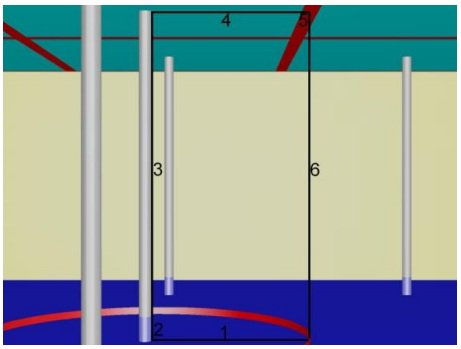


**Figure 3** Close view of the zone of influence around a diffuser.

However, a certain distance downstream the diffuser, the perforations have no influence on the flow, as shown in Figure 4, where the dimensionless velocity profiles are compared along four vertical lines at different radial distances from two different diffusers: one with perforations and the other without them. The dimensionless velocity used is defined as:

$$v^* = \frac{|v|}{v_s \frac{A_{eff}}{A_l}}, \qquad (1)$$

where $v^*$ is the dimensionless velocity, $v_s$ is the mean air velocity at the diffuser exit, $|v|$ is the magnitude of the air velocity, $A_{eff}$ is the effective area of the lateral face the air goes through, and $A_l A_l$ is the total area of that face. In the diffuser with no perforations $A_{eff}$ is equal to $A_l$. Therefore, in Figure 4, on the one hand, the solid lines correspond to the velocity profiles of a diffuser with the lateral plate cut in strips of 1 cm so, alternately, it supplies air or not in order to simulate the effect of the perforated plate. While, on the other hand, the dotted lines correspond to the velocity profiles of a diffuser whose lateral face is completely of air discharge. As can be seen in Figure 4, 5 cm downstream the diffuser ($r$=$D$/2+0.04 m), the oscillations produced by the perforations are damped and the obtained profiles using both diffusers are quite similar. Therefore, the computational cost will be reduced by using the diffuser without perforations and the results will be practically the same than when a perforated diffuser is used. Thus, a diffuser whose lateral face is completely discharging air is the one used to numerically characterize the problem under study.

In order to discretize the computational domain, a structured mesh of quadrilaterals elements is used in the simulations. The elements are compressed in the region close to the floor to properly resolve the boundary layer. The grid independence was examined by solving the flow field using three different mesh configurations with 15,476, 45,441 and 84,992 cells. Practically, the same results were obtained with the two finer meshes, as shown in Figure 5, which depicts the vertical profiles of velocity magnitude, temperature and turbulence intensity at $r$ = 3 m. On the other hand, since the quality of the mesh plays an important role in the stability and accuracy of numerical calculations, it is necessary to reach a compromise between accuracy and computational cost. Therefore, the mesh of 45,441 cells is chosen for the simulation: the use of the finest mesh only would increase the computational time.

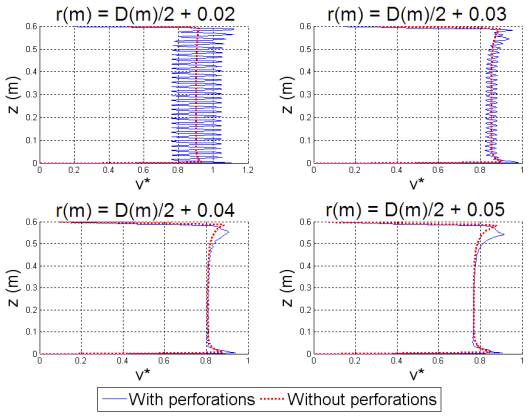


**Figure 4** Dimensionless profile of the velocity magnitude along vertical lines in the radial positions indicated.

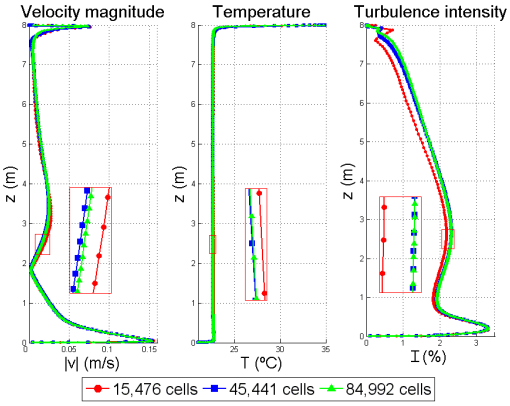


**Figure 5** Grid independence study. A zoom view of the region inside the red rectangle is also included.

Regarding the boundary conditions used in the simulations, they are described in detail in Table 1. The location of the corresponding boundary condition can be checked with the corresponding number in the sketch of the computational domain shown in Figure 3.

| | |
|---|---|
| 1<br>Floor | -Type: wall<br>-Area: 54.0354 m$^2$<br>-Temperature: 17 – 19 – 21ºC<br>-Density: 2,500 kg/m$^3$<br>-Specific heat: 1,000 J/kg K<br>-Thermal conductivity: 2.3 W/m K |
| 2<br>Supply | -Type: mass-flow-inlet<br>-Area: 0.57 m$^2$ |

| | |
|---|---|
| | -Mass flow-rate: 0.4 kg/s<br>-Temperature: 19 – 21 – 23ºC<br>-Direction: normal to boundary<br>-Turbulence intensity: 4.55%<br>-Hydraulic Diameter: 0.6 m |
| 3<br>Air tube connection | -Type: wall<br>-Area: 6.97 $m^2$<br>-Heat flux: 0 $W/m^2$ (adiabatic)<br>-Density: 2,719 $kg/m^3$<br>-Specific heat: 871 J/kg K<br>-Thermal conductivity: 202.4 W/m K |
| 4<br>Ceiling | -Type: wall<br>-Area: 48.946 $m^2$<br>-Temperature: 35ºC<br>-Density: 2,000 $kg/m^3$<br>-Specific heat: 750 J/kg K<br>-Thermal conductivity: 1.4 W/m K |
| 5<br>Exhaust | -Type: pressure-outlet<br>-Area: 5.0894 $m^2$<br>-Gauge pressure: 0 Pa<br>-Backflow total temperature: 35 ºC<br>-Backflow Direction: from neighboring cell |
| 6<br>Symmetry | -Type: symmetry<br>-Area: 208.6 $m^2$ |

**Table 1** Boundary conditions.

## PHYSICAL AND NUMERICAL CONSIDERATIONS

The airflow pattern and temperature distribution in the enclosure are governed by the conservation laws of mass, momentum and energy. The flow is assumed to be axisymmetric, steady-state and turbulent with buoyancy effects taken into account. The radiation heat transfer was not included in the model. The air was modelled as an ideal gas.

Regarding the turbulent model, the two-equation k-ε RNG (Re-Normalization Group) model [13] was employed in this study. This model is a very reliable and a commonly used CFD model for assessment of indoor thermal conditions, as well as it has been used to simulate the thermal environment in large space buildings [14] where good agreement between numerical and experimental results were found. Finally, Upwind Second-Order scheme and SIMPLE algorithm were used for space discretization and Pressure-Velocity coupling in the numerical simulations, respectively.

## CFD SIMULATION RESULTS

This section is dedicated to present the thermal conform results depending on the occupancy level of the enclosure. To start with, we shall take into account that there are not thermal loads due to, for instance, human bodies and a optimal configuration, in terms of the DV air stream angle, and both DV and RCF temperature, will be obtain. After that, the effect of having thermal loads uniformly distributed in the domain will be taken into account.

### WITHOUT THERMAL LOADS BY OCCUPANTS

#### Buoyancy effect

In displacement ventilation, with air low drive speeds, it is necessary to study the phenomena of buoyancy to perform an optimum design of the installation. To do this, the Archimedes dimensionless number is employed. This number represents the ratio of buoyancy to inertial forces and is defined as:

$$Ar = \frac{\beta\ g\ L_c\ \Delta T_{s-f}}{{v_s}^2}, \qquad (2)$$

where $\beta$ is the coefficient of thermal expansion, $g$ the gravity, $\Delta T_{s-f}$ the temperature difference between the air supplied by the diffuser and the floor surface, and $v_s$ the mean air velocity at the diffuser exit. The characteristic length ($L_c$) of the problem is related to the effective area of the diffuser as:

$$L_c = \left(A_{eff}\right)^{1/2} = \left(K\ 2\pi\ \frac{D}{2}\ h\right)^{1/2}. \qquad (3)$$

To check the buoyancy effects, three simulations were performed with different Archimedes numbers: 2.84 ($Ar$ >1, for which upward buoyancy forces are dominant), 0.41 (-1< $Ar$ >1, for which inertial forces are dominant) and -2.91 (for which downward buoyancy forces are dominant). In Figure 6, contours of the steady state velocity field in the three simulations are compared. It shows that for $Ar$ >1, left subfigure, the air stream is not driven away from the diffuser and it directly rises to the upper region of the enclosure. On the contrary, for $Ar$ <1, middle and right subfigures, it is clear that the air stream is able to cover the entire bottom of the occupied zone, creating a strip of cold air in the lower part of the enclosure. The air displacement ventilation is based on moving the cold air along the ground in the occupied zone, and when it contacts with heat sources, increases its temperature and goes upward to the top of the enclosure. Therefore after this first study we can say that to achieve the most effective ventilation, the floor temperature and supplied air velocity and temperature must be selected such that $Ar$ <1.

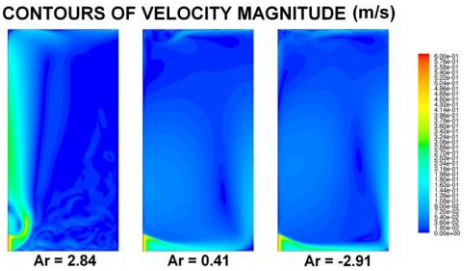


**Figure 6** Bouyancy effect of the various Archimedes number.

#### Effect of air discharge angle

The closer to the floor the air moves, the lesser the discomfort it generates. To check this effect 9 simulations were made with different air supply angles ($\alpha$): +15º, 0º to -15º and injecting the air at three temperatures: 19, 21 and 23 ºC.

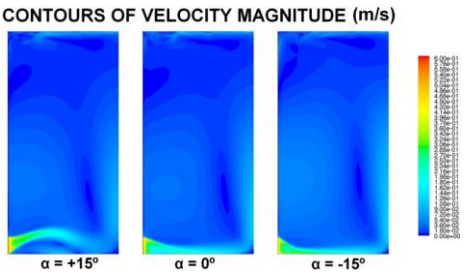


**Figure 7** Effect of air discharge angle.

Figure 7 shows the velocity profiles when the air is supplied at 21 ºC. It shows, how positive angles, left figure, will give place to air currents that will generate thermal discomfort. By injecting air with negative angles, right figure, the movement of the cold air will take place at floor level and a greater surface will be covered. Almost the same effect is observed when the injecting angle is zero, central figure, so this angel will be final chosen one for the remaining simulations since commercial diffusers cannot change their air discharge angles and it is 0º.

**Effect of supplied air temperature and floor temperature**

In this section, 9 more simulations were performed in order to limit the range of values for the supplied air temperature and floor temperature. In the simulations, three different supplied air temperatures were chosen: 19, 21, and 23 ºC, while for the floor it was used: 17, 19, and 21 ºC. Figure 8 shows radial profiles of the indices defined in ISO 7730 (PMV, PPD, Draught rate, Vertical difference temperature, Cool floor and Radiant asymmetry), for the case with the floor at 19 ºC and the supplied air at 23 ºC. The horizontal red, green and blue dash lines delimit the range of values each parameter must have in order to achieve the enclosure the thermal classification of Category A, B and C, respectively. Ideally, to achieve the classification of category A all indices must be within the range of values defined by the dashed red lines. Additionally, it is necessary to clarify that, as indicated in ISO 7730, the occupation zone begins one meter far from the wall of the diffuser. Therefore, Figure 8 and following must be analyzed from $r$ = 1.15 m = $D$/2 + 1 m, without being important what happens for lower radial positions.

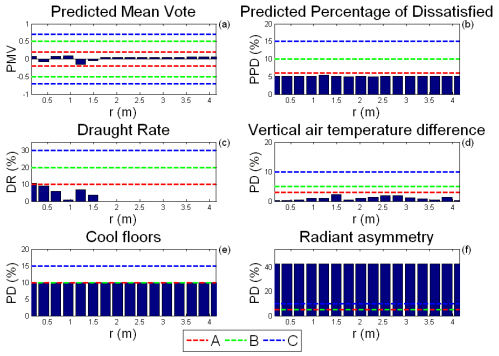


**Figure 8** Indices of ISO 7730. Supplied air is at 23 ºC and floor surface at 19 ºC.

PMV and PPD indices, Figure 8 (a) and (b), respectively, indicate that by supplying air at 23 °C, the thermal sensation is almost neutral and the classification of the thermal environment, according with these indices, can be Category A. However, we shall show that if a heat produced by occupants were taken into account, it would be necessary to supply the air at a slightly lower temperature.

Local discomfort indices due to draught and vertical air temperature difference, Figure 8 (c) and (d), show that the hybrid cooling system provides a high degree of comfort to the enclosure, since it does not generate uncomfortable drafts or excessive vertical temperature gradients. According to these indices the classification of Category A is reached, too.

Regarding the index of local discomfort due to the presence of a cold floor, Figure 8 (e), with the floor temperature at 19 °C, the classification of Category A is also achieved. If the floor were kept at 17 °C, the classification would be Category C (not shown).

Finally, the radiant temperature asymmetry index, Figure 8 (f), is out the classification. The radiant temperature asymmetry index is given exclusively by the temperatures of the ceiling and floor. According to this index, the classification of Category A requires a temperature difference below 5 ºC between both surfaces. However, this difference is not possible without a support system to cool the ceiling but, in that case, the advantage of dealing only with thermal loads in occupied zone is missed. It is also probably that a temperature difference above 5 °C in a high-rise enclosure does not generate the discomfort indicated by ISO 7730, as noted in [15]-[16]. Therefore, the applicability of this index is brought into question, because as indicated in [17] the model to calculate the radiant asymmetry in standard ISO 7730 was derived from laboratory-based measurements conducted in the mid-1960s in relatively conventional environments while DV + RCF represents a more sophisticated environment.

**WITH THERMAL LOADS BY OCCUPANTS**

The drawback of 2D axisymmetric simulations is the inability to model a located heat source, as a human person or a computer. So in this section, the thermal load is simulated as a volumetric load uniformly distributed within the occupied zone, with a value of 22 W/m$^3$, equivalent to an occupancy level of 3 m$^2$/pers with a metabolic rate of 1.2 met (69.84 W/m$^2$). Again, 9 new simulations were performed. In the simulations, now with the volumetric heat load, three different temperatures are chosen for the supplied air: 19, 21, and 23 °C and also three for the floor: 17, 19, and 21 °C. The radial evolution of the thermal comfort indices is shown in Figure 9, where one can see how the indices measuring the discomfort due to both Vertical air difference temperature and Radiant asymmetry, Figure 9 (d) and (f), respectively, are out of any category. On the one hand, as commented above, the Radiant asymmetry is impossible to reduce unless the ceiling temperature was reduced.

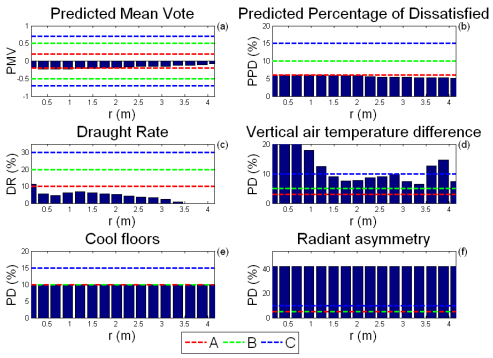


**Figure 9** Indices of ISO 7730. Suplied air at 19 ºC and floor surface at 19 ºC.

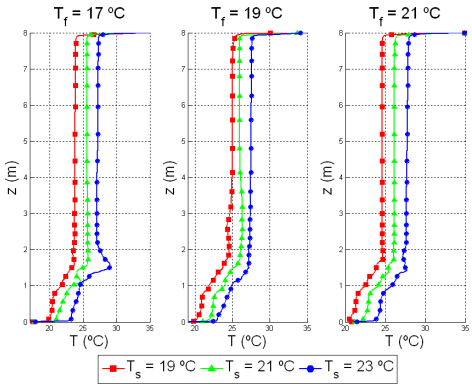


**Figure 10** Vertical air temperature profile.

On the other hand, for this configuration of parameters, Figure 10 shows the vertical air temperature profiles along the vertical line for $r$ = 3 m. From them one can observe that the vertical temperature gradient in the occupied zone is greater than 2°C/m and this is reason of the discomfort observed in Figure 9 (d). One solution to this problem could be achieved by selecting a higher diffuser looking for that fresh air was introduced into the occupied zone more uniformly. Therefore, a new diffuser 2 m high and with a diameter of 0.81 m was study.

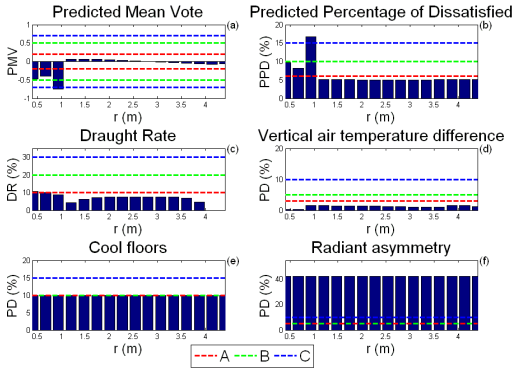


**Figure 11** Indices of ISO 7730. Suplied air at 19 ºC and floor surface at 21 ºC.

The radial evolution of the thermal comfort indices is shown in Figure 11. As can be seen, the percentage of discomfort due to vertical air temperature difference is reduced and with the new diffuser the classification of Category A is achieved. The values of the indices from $r$ = 0 to 1.405 m ($D$/2+1 m) are outside of the occupied zone and do not affect to determine the classification.

## CONCLUSIONS

It has been shown that a system of cooling DV + RCF has certain advantages over a conventional cooling system: it allows reducing the operating temperature which causes a stratification of cold air in the occupied zone, reduces the transfer of infrared energy from the upper enclosure to the occupied zone, without compromising the thermal comfort conditions. It is also noteworthy that bigger diffusers improve air distribution in the occupied zone and were able to reduce discomfort due to vertical air temperature difference.

Another issue to be taken care in future research is the applicability of the radiant temperature asymmetry index if hybrid systems DV + RCF were used.

## REFERENCES

[1] World Health Organization. Indoor air pollutants: exposure and health effects. EURO Reports and Studies Nº 78, WHO Regional Office for Europe. Copenhagen 1983.

[2] Directive 2002/91/CE of the European Parliament and of the Council of 16 December 2002 on the energy performance of buildings, 2002.

[3] Air quality guidelines for Europe. World Health Organization, Copenhagen (2000).

[4] Z. Lin, T.T. Chow, K.F. Fong, Q. Wang, Y. Li. Comparison of performances of displacement and mixing ventilations. Part I: thermal comfort. International Journal of Refrigeration, Vol. 28, 2005, pp. 276–287.

[5] Z. Lin, T.T. Chow, K.F. Fong, C.F. Tsang, Q. Wang. Comparison of performances of displacement and mixing ventilations. Part II: indoor air quality. International Journal of Refrigeration, Vol. 28, 2005, pp. 288–305.

[6] D. Song, T. Kim, S. Song, S. Hwang, S.B. Leigh. Performance evaluation of a radiant floor cooling system integrated with dehumidified ventilation. Applied Thermal Engineering, Vol. 28, 2008, pp. 1299–1311.

[7] F. Causone, F. Baldin, B.W. Olesen, S.P. Corgnati. Floor heating and cooling combined with displacement ventilation: Possibilities and limitations. Energy and Buildings, Vol. 42, 2010, pp. 2338–2352.

[8] ISO 7730:2005. Ergonomics of the thermal environment. Analytical determination and interpretation of thermal comfort using calculation of the PMV y PPD indices and local thermal comfort criteria.

[9] Q. Li, H. Yoshino, A. Mochida, B. Lei, Q. Meng, L. Zhao, Y. Lun. CFD study of the thermal environment in an air-conditioned train station building. Buildings and Environment, Vol. 4, 2009, pp. 1452–1465.

[10] W. Kessling, S. Holst, M. Schuler. Innovative Design Concept for the New Bangkok International Airport, NBIA. *Symposium on Improving Building Systems in Hot and Humid Climates*. Dallas 2004.

[11] FLUENT 6.3 User's Guide (2006).

[12] J.M. Peña-Suárez & J. Ortega-Casanova. Computational fluid dynamics characterization of a hibrid cooling system composed of a displacement ventilation unit and radiant cooling floor. *Computational Thermal Sciences*, vol. 5(2) 2013, pp 127-141.

[13] V. Yakhot, S.A. Orszag. Renormalization group analysis of turbulence. I. Basic theory. *Journal of Scientific Computing*, Vol. 1, 1986, pp. 3–51.

[14] P. Rohdin, B. Moshfegh. Numerical predictions of indoor climate in large industrial premises – a comparison between different k–ε models supported by field measurements. *Building and Environment*, Vol. 42, 2007, pp. 3872–82.

[15] G. Langkilde, L. Gunnarsen, N. Mortensen, 1985. Comfort limits during infrared radiant heating of industrial spaces. *CLIMA 2000*, Copenhagen.

[16] Z. Wang, H. Zhang, E. Arens, D. Lehrer, C. Huizenga, T. Yu, S. Hoffman. Modeling thermal comfort with radiant floors and ceilings. *4th International Building Physics Conference* 2009, June 15-18, Istanbul.

[17] D. L. Loveday, K. C. Parsons, A. H. Taki, S. G. Hodder. Displacement ventilation environments with chilled ceilings: thermal comfort design within the context of the BS EN ISO7730 versus adaptive debate. *Energy and Buildings* 34 (2002) 573–579).